Development 138, 3055-3066 (2011) doi:10.1242/dev.063214

Msx genes define a population of mural cell precursors required for head blood vessel maturation

Miguel Lopes[1], Olivier Goupille[1,*], Cécile Saint Clement[1], Yvan Lallemand[1], Ana Cumano[2] and Benoît Robert[1,†]

SUMMARY

Vessels are primarily formed from an inner endothelial layer that is secondarily covered by mural cells, namely vascular smooth muscle cells (VSMCs) in arteries and veins and pericytes in capillaries and veinules. We previously showed that, in the mouse embryo, *Msx1*^{lacZ} and *Msx2*^{lacZ} are expressed in mural cells and in a few endothelial cells. To unravel the role of Msx genes in vascular development, we have inactivated the two Msx genes specifically in mural cells by combining the *Msx1*^{lacZ}, *Msx2*^{lox} and *Sm22α-Cre* alleles. Optical projection tomography demonstrated abnormal branching of the cephalic vessels in E11.5 mutant embryos. The carotid and vertebral arteries showed an increase in caliber that was related to reduced vascular smooth muscle coverage. Taking advantage of a newly constructed *Msx1*^{CreERT2} allele, we demonstrated by lineage tracing that the primary defect lies in a population of VSMC precursors. The abnormal phenotype that ensues is a consequence of impaired BMP signaling in the VSMC precursors that leads to downregulation of the metalloprotease 2 (*Mmp2*) and *Mmp9* genes, which are essential for cell migration and integration into the mural layer. Improper coverage by VSMCs secondarily leads to incomplete maturation of the endothelial layer. Our results demonstrate that both Msx1 and Msx2 are required for the recruitment of a population of neural crest-derived VSMCs.

KEY WORDS: Msx, BMP, Neural crest, Mouse

INTRODUCTION

The cardiovascular system is composed of the heart, arteries, arterioles, capillaries, veinules and veins. Two distinct layers compose the blood vessels: the inner endothelium and the external mural layer. Endothelial cell (EC) assembly takes place first. Within the mouse embryo, mesodermal progenitors give rise to the angioblast, an endothelial precursor. The angioblasts start to aggregate as early as embryonic day (E) 7.5, forming the ventral and dorsal aortas as well as the vitelline vascular tree. The expansion and specialization of this initial basic system is achieved by angiogenesis, involving EC sprouting, vessel branching and intussusception from existing blood vessels (Risau, 1997).

Vascular maturation then takes place and confers endothelial tube contractility and resistance (Jain, 2003). Its primary mediators are the mural cells that form a multi-layered vascular smooth muscle around arteries and veins, whereas in capillaries and veinules the mural layer is composed of sparse pericytes. These mural cells originate from different sources depending on their position within the body. Most vascular smooth muscle cells (VSMCs) of the head and aortic arch have a neural crest origin (Jiang et al., 2000; Etchevers et al., 2001; Korn et al., 2002) (for a review, see Majesky, 2007), whereas those of the trunk primarily derive from the somitic and lateral plate mesoderm (Esner et al., 2006; Majesky, 2007; Santoro et al., 2009; Wiegreffe et al., 2009). Vascular maturation further involves the development of an elastic lamina between endothelial cells and VSMCs and of an extracellular matrix (ECM) that embeds both layers (Jain, 2003).

Vascular maturation involves the proliferation, migration and differentiation of VSMCs. These are orchestrated by multiple signaling pathways, including PDGFβ/PDGFRβ (Hellstrom et al., 1999), TGFβ (Majack, 1987; Battegay et al., 1990; Nishishita and Lin, 2004), angiopoietin 1 (Angpt1)-Tie2 (Fukuhara et al., 2008; Saharinen et al., 2008) and BMP (El-Bizri et al., 2008; Spiekerkoetter et al., 2009; Bai et al., 2010).

In the mouse, the Msx gene family is composed of three homeodomain transcription factors. Msx1 and Msx2 play important and often overlapping roles in the development of craniofacial structures, neural tube and limb (Alappat et al., 2003; Bach et al., 2003; Lallemand et al., 2009). In humans, *MSX1* mutations lead to cleft palate and lips, as well as to tooth agenesis (Vastardis et al., 1996; Kapadia et al., 2007). *MSX2* has been associated with craniosynostosis (Wilkie, 1997). *Msx3* is absent from the human genome (Finnerty et al., 2009) and in the mouse its expression is restricted to the dorsal aspect of the neural tube (see Ramos and Robert, 2005).

Recently, we have shown that in the adult mouse, both *Msx1* and *Msx2* are expressed in a subset of peripheral artery VSMCs. Furthermore, *Msx1* is expressed in pericytes of capillaries and *Msx2* in ECs of the dorsal aorta. In the embryo, both *Msx1* and *Msx2* are detected in some ECs of the aorta from E14.5 and *Msx1* additionally in mural cells of the intersomitic arteries from E10.5 (Goupille et al., 2008). We have undertaken the present study to clarify the role of Msx genes in vascular development. Phenotypic analyses and gene expression assays demonstrate that VSMC coverage is reduced in the *Msx1*$^{-/-}$*; Msx2*$^{lox/-}$*; Sm22α-Cre* mutant (hereafter referred to as *Sm22Cre Msx1/2*), resulting in an increase in vessel diameter and impairment of endothelium maturation. By genetic lineage tracing, we show that the primary defect lies in a

[1]Institut Pasteur, Génétique Moléculaire de la Morphogenèse, CNRS URA 2578, F-75015 Paris, France. [2]Institut Pasteur, Développement des Lymphocytes, INSERM U668, F-75015 Paris, France.

*Present address: Commissariat à l'Energie Atomique, 18 route du Panorama, BP6 92265 Fontenay aux Roses cedex, France
†Author for correspondence (benoit.robert@pasteur.fr)

Accepted 4 May 2011

population of VSMC precursors. BMP signaling and its targets *Mmp2* and *Mmp9* are downregulated in *Msx1; Msx2* mutant VSMCs, leading to impaired incorporation of *Msx1*-expressing vascular smooth muscle precursors into the mural layer.

MATERIALS AND METHODS

Mice

We previously reported the generation of *Msx1* null (*Msx1*^{lacZ}), *Msx2* null (*Msx2*^{GFP}, *Msx2*^{lacZ}) and conditional (*Msx2*^{lox}) mutant alleles (Houzelstein et al., 1997; Lallemand et al., 2005; Bensoussan et al., 2008). The *Msx1*^{lox} conditional mutant allele (Fu et al., 2007) was a generous gift from Dr Robert Maxson (Los Angeles, CA, USA) and the *Tie2-Cre* transgenic mouse (Kisanuki et al., 2001) from Dr Masashi Yanagisawa (Dallas, TX, USA). The *Sm22α-Cre* (Zhang et al., 2006) and *Rosa*$^{mT/mG}$ (Muzumdar et al., 2007) engineered mice were purchased from The Jackson Laboratory (Bar Harbor, ME, USA). The *Msx1*^{CreERT2} mouse was generated by introducing the CreERT2 coding sequence (Feil et al., 1996) (a kind gift of Pierre Chambon, Illkirch, France) at the initiator ATG site of *Msx1* by homologous recombination in ES cells. *CreERT2* interrupts the *Msx1* coding sequence, thus creating a null allele. After Southern blot selection, recombinant cells were injected into blastocysts and these were reimplanted using standard protocols. All mice were maintained on an NMRI outbred background. Genotyping primers are listed in Table S1 in the supplementary material. All studies were conducted using mutant embryos with littermates as controls.

Administration of Tamoxifen to *Msx1*^{CreERT2} mice

Tamoxifen (Sigma) was dissolved in ethanol, emulsified in sunflower oil (Sigma) and then sonicated three times for 5 seconds each at a final concentration of 10 mg/ml. Tamoxifen was intraperitoneally injected either three times at 3.5 mg per injection or twice at 2.5 mg per injection per pregnant female (weight, 30 g). Successive injections were performed at 12-hour intervals.

Optical projection tomography (OPT)

Embryos were fixed overnight in 4% paraformaldehyde and non-specific epitopes blocked overnight in 0.1% sodium azide, 1 mM $MgCl_2$, 1% BSA, 10% goat serum, 0.5% Triton X-100 and 0.5% Tween 20. A 1-week incubation with rat anti-mouse CD31 (BD Pharmingen) antibody was performed followed by a 5-day incubation with a secondary anti-rat antibody (Alexa 546, Invitrogen). Acquisition and treatment of images using OPT was performed by Bioptonics MRC Technology (Edinburgh, UK) according to published protocols (Sharpe et al., 2002).

Quantitative real-time PCR (qRT-PCR) on dissected embryonic cephalic tissues

RNA was extracted using the RNeasy Mini Extraction Kit (Qiagen). RT-PCR was performed on a StepOnePlus machine (Applied Biosystems, Warrington, UK) using SYBR PCR Master Mix (Applied Biosciences). Primers are listed in Table S2 in the supplementary material. *Gapdh* was used as a reference. PCR efficiency was in the range 98-100% for all assays. PCR cycle parameters were: 10 minutes at 95°C initial incubation, followed by 15 seconds at 95°C and 1 minute at 60°C for 40 cycles. For each gene studied, multiple RNA samples were analyzed; *n*=5 for single *Msx1* and single *Msx2* mutants, *n*=4 for *Sm22Cre Msx1/2* mutants, each in duplicate. Data are expressed as fold changes [$2^{-(\Delta ctmutant-\Delta ctreference)}$] using *Msx1*$^{+/-}$*; Msx2*$^{lox/+}$*; Sm22α-Cre* triple heterozygotes as a reference.

In situ hybridization

E11.5 embryos were fixed for 2 hours in 4% paraformaldehyde (Sigma) then immersed in 15% sucrose and O.C.T. Compound (Tissue-Tek) before being frozen in liquid nitrogen and cryostat sectioned at 20 μm. The *Bmp4* probe was a gift from Dr B. Hogan (Durham, NC, USA). Automated in situ hybridizations were performed with an InsituPro VSi apparatus (Intavis Bioanalytical Instruments, Köln, Germany).

Immunohistochemistry

Immunohistochemistry was performed as described (Goupille et al., 2008) except that X-Gal staining was omitted. Primary antibodies are listed in Table 1. Secondary antibodies (Invitrogen) were: Alexa Fluor 488 goat anti-mouse and goat anti-rabbit, Alexa Fluor 568 goat anti-rabbit, Alexa Fluor 647 goat anti-mouse and Alexa Fluor 635 goat anti-rabbit at 1/300 and Alexa Fluor 488 streptavidin at 1/1000. A Zeiss Axioplan microscope equipped with an Apotome and with Axiovision software (Carl Zeiss, Jena, Germany) was used for vessel section surface measurements. All images were assembled in Photoshop and Illustrator (Adobe Systems, San Jose, CA, USA).

Flow cytometry

The E12.5 embryos used were either heterozygous or homozygous at the *Sm22α-Cre; Rosa*$^{mT/mG}$*; Msx1*^{lacZ}*; Msx2*^{lacZ} loci. They were genotyped before cell dissociation. Cells were dissociated mechanically with a 1-ml 26 gauge syringe and resuspended in Dulbecco's Modified Eagle's Medium (Invitrogen) containing 2% fetal bovine serum (Invitrogen). VSMCs were sorted on the basis of *GFP* expression. For ECs, the cell suspension was labeled with Phycoerythrin-conjugated anti-CD31 antibodies (BD Biosciences). Cells were then washed with PBS and fluorescence was quantified as relative fluorescence units on a MoFlo High Performance Cell Sorter (Beckman Culture, Krefeld, Germany). Values are reported as mean fluorescence units.

In vitro assays

VSMCs were FACS sorted as described above and maintained in DMEM supplemented with 10% fetal bovine serum and streptomycin on collagen I (BD Biosciences)-coated plates. The medium was changed every 48 hours and cells were passaged a maximum of six times (i.e. up to 20 days) using accutase digestion (Gibco). Recombinant mouse Bmp4 (Roche) was added to *Msx1*$^{-/-}$*; Msx2*$^{-/-}$ cells and these were incubated for a further 48 hours, then lysed and RNA extracted using the RNeasy Mini Extraction Kit (Qiagen). *Msx1*$^{+/-}$*; Msx2*$^{+/-}$ cells were transfected with *Msx1* and *Msx2* small interfering RNA (siRNA; siGENOME SMARTpool, Dharmacon) and with siGLO Risc-Free control siRNA (Dharmacon) as a control for transfection efficiency. DharmaFECT transfection reagent (Dharmacon) was used according to the manufacturer's instructions. After 48 hours, cells were lysed and RNA extracted as described above.

Table 1. Primary antibodies

Antibody	Source	Dilution
Monoclonal rat anti-mouse α-SMA Cy3 conjugate	Sigma	1/1000
Polyclonal rabbit anti-mouse Pdgfrβ	Santa Cruz	1/200
Monoclonal rat anti-mouse CD31 biotin coupled	BD Pharmingen	1/100
Monoclonal rat anti-mouse CD31	BD Pharmingen	1/100
Polyclonal rat anti-mouse CD144 (Cdh5)	BD Pharmingen	1/100
Polyclonal rabbit anti-mouse Tie2	Santa Cruz	1/200
Polyclonal rabbit anti-β-galactosidase	Cappel	1/1500
Monoclonal rabbit anti-mouse GFP	Invitrogen	1/500
PE rat anti-mouse CD31	BD Pharmingen	1/400
Monoclonal mouse anti-mouse GFP	Chemicon	1/500

With the exception of the Phycoerythrin (PE) rat anti-mouse CD31 antibody, which was used only in flow cytometry, all antibodies were used for immunohistochemistry on embryo sections. The monoclonal rat anti-mouse CD31 was also used to perform OPT.

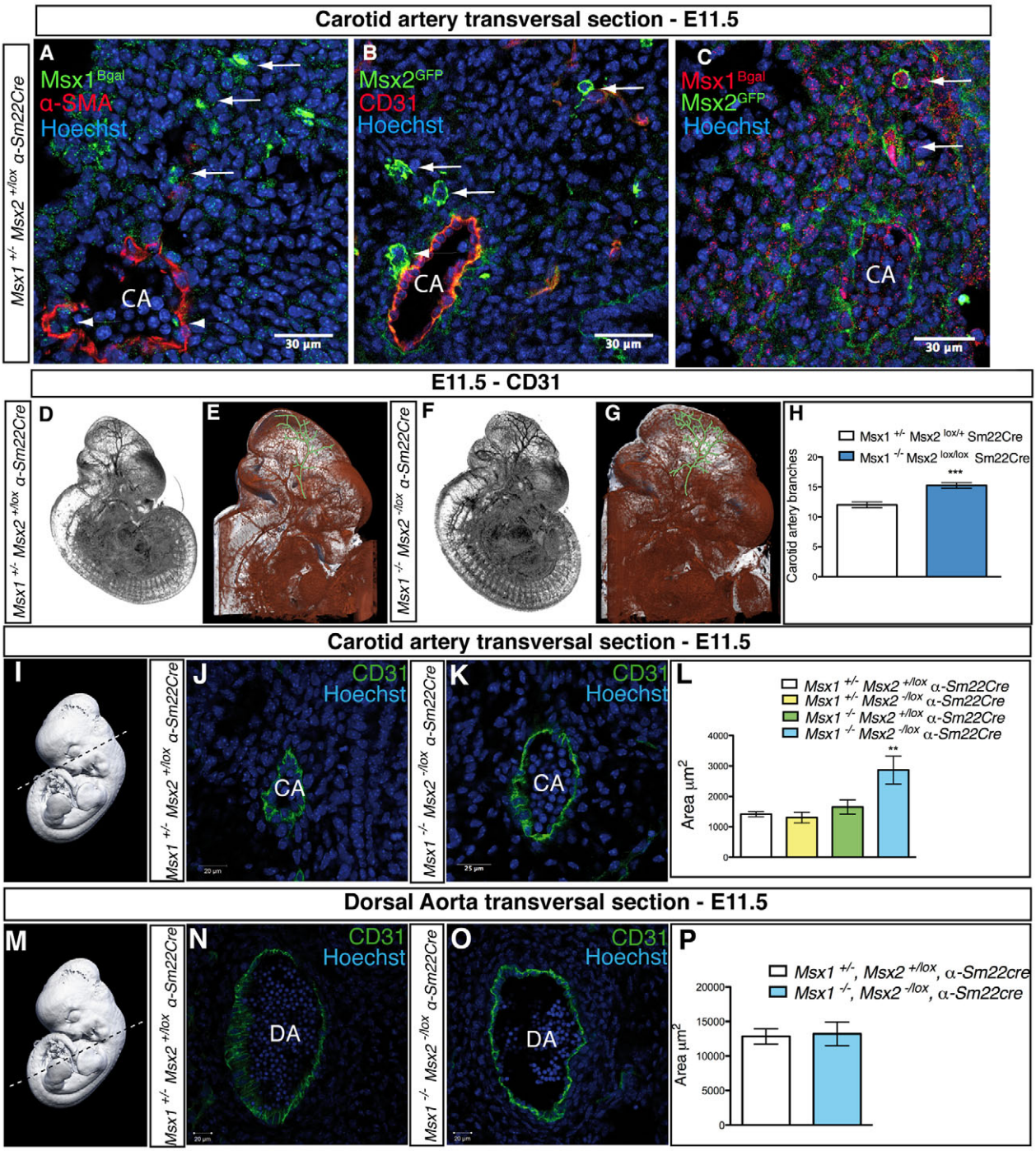

Fig. 1. Overbranching and caliber increase of the carotid artery in Msx mutants. (**A-C**) Transverse sections of E11.5 mouse embryo heads reveal expression of *Msx1*^{lacZ} in inner endothelial cells (ECs) of the carotid artery (CA) (A, arrowheads) as well as in external mesenchymal cells (A, arrows). *Msx2*^{GFP} is expressed in vascular smooth muscle cells (VSMCs) (B, arrowheads) as well as in some external mesenchymal cells (B, arrows) that may also express *Msx1*^{lacZ} (C, arrows). (**D-G**) Extra branching of the CA identified by optical projection tomography (OPT). At low magnification, where the whole embryonic vasculature is visible, the *Sm22Cre Msx1/2* mutant embryos (F) show major vascular alterations in the head as compared with controls (D). Magnified images confirm the increase in branching density from the CA in the *Sm22Cre Msx1/2* mutant (G) as compared with the control (E). The CA and its major branches are highlighted in green. (**H**) Primary and secondary branch quantification from the right and left CA of the embryos in D-G. For each genotype, n=3; ***, P<0.001 (non-parametric Dunnett test). (**I-P**) Measure of the section surface of the CA (I-L) and dorsal aorta (DA) (M-P), both visualized by the endothelial marker CD31 (green) on transverse sections at E11.5. The section planes (dashed lines) are shown for the CA (I) and DA (M). In the *Sm22Cre Msx1/2* mutant, the CA (K) section surface is increased compared with the control (J). By contrast, the DA surface area is not significantly different in the mutant (O) and control (N). Average area quantification is shown for the CA (L) and DA (P). For each genotype, n=8; **, P<0.01 (non-parametric Dunnett test). Error bars indicate s.e.m. Scale bars: 30 µm in A-C; 25 µm in K; 20 µm in J,N,O.

Statistical analysis

For results from qRT-PCR, diameter measurements and cell number quantification, means ± s.e.m. were calculated. For qRT-PCR experiments, results from Msx mutant analysis were expressed as fold change relative to Msx double-heterozygous littermates or as absolute values. Cell counts and area measurements were performed using ImageJ version 1.43g (NIH). One-way ANOVA was used to compare independent experiments. Comparison between data groups was performed using a non-parametric Dunnett test. All statistical analyses were performed using GraphPad Prism version 5.0 for Apple (GraphPad software, San Diego, CA, USA).

RESULTS

Msx1 and *Msx2* expression in the mouse embryo head vessels and mutation strategy

We previously demonstrated that, in the adult mouse, *Msx1* and *Msx2* are expressed in the VSMCs of peripheral arteries (Goupille et al., 2008). In E11.5 embryos, $Msx1^{lacZ}$ was detected in a few ECs of the carotid artery (CA) (Fig. 1A). $Msx1^{lacZ}$ expression was also observed in mesenchymal cells outside the CA, some of which co-expressed $Msx2^{GFP}$ (Fig. 1C). $Msx2^{GFP}$ was mainly expressed in differentiated VSMCs of the CA (Fig. 1B). At E12.5, $Msx1^{lacZ}$ was detected mainly in the endothelial layer of the CA and vertebral artery (VA) but not in veins (see Fig. S1 in the supplementary material). Expression of $Msx1^{lacZ}$ was also observed in a few cells of the most external VSMC layer, and again in mesenchymal cells further away from the CA (see Fig. S1 in the supplementary material). $Msx2^{GFP}$ expression was maintained in the VSMCs at this stage.

To inactivate both genes in blood vessels, we combined a null (Lallemand et al., 2005) and a floxed (Bensoussan et al., 2008) *Msx2* allele and the *Sm22α-Cre* (*Sm22α* is also known as transgelin – Mouse Genome Informatics) transgene (Zhang et al., 2006), together with $Msx1^{lacZ}$ null alleles. Using this strategy, *Msx1* is inactivated in the two layers of the blood vessel, whereas *Msx2* is inactivated only in the VSMCs. The *Sm22α-Cre* transgene that we used was chosen to inactivate $Msx2^{lox}$ because of its early activation in mural cells (El-Bizri et al., 2008). The $Rosa^{mT/mG}$ allele ubiquitously produces a membrane-bound Tomato red fluorescent protein, which is replaced by membrane-bound GFP after Cre-mediated recombination (Muzumdar et al., 2007). When associated with this allele, the *Sm22α-Cre* transgene drives expression of GFP in VSMCs at embryonic stages before they integrate into the CA and, consequently, before they express differentiation markers such as alpha-smooth muscle actin (α-*Sma*; *Acta2* – Mouse Genome Informatics) (see Fig. S2 in the supplementary material). *Sm22Cre Msx1/2* mutants die a few hours after birth due to *Msx1* deficiency (Houzelstein et al., 1997), in contrast to constitutive double mutants that die at E14.5 (Lallemand et al., 2005).

Inactivation of *Msx1* and *Msx2* in the VSMC lineage, but not the endothelium, leads to defects in head vascularization

By optical projection tomography (OPT), we first observed overbranching of the CA at E11.5 in the *Sm22Cre Msx1/2* mutant (Fig. 1D-G; see Movies 1 and 2 in the supplementary material) but not in the *Msx1* or *Sm22Cre Msx2* single mutants (data not shown). The number of primary and secondary CA branches was increased by ~1.4-fold in the mutant (Fig. 1H). No branching defect was detected in capillaries by immunofluorescence on sections (data not shown). Furthermore, a 2-fold increase in arterial caliber was observed in the *Sm22Cre Msx1/2* mutant. At E11.5, the CA section surface increased from ~1400 μm^2 in the control to ~2900 μm^2 in the mutant (Fig. 1I-L). The VA caliber was also increased (data not shown). No change was observed in single *Msx1* or *Sm22Cre Msx2* mutants. In contrast to the CA, no significant change was observed in dorsal aorta sections of the double mutant (~13,200 μm^2) relative to the control (~12,800 μm^2) (Fig. 1M-P).

Strikingly, quantification of α-SMA-positive cells in the CA revealed a halving in the number of VSMCs in the double mutant (Fig. 2A,D) as compared with the control (Fig. 2G). RNA was extracted from heads of E11.5 embryos (Fig. 2H) and the

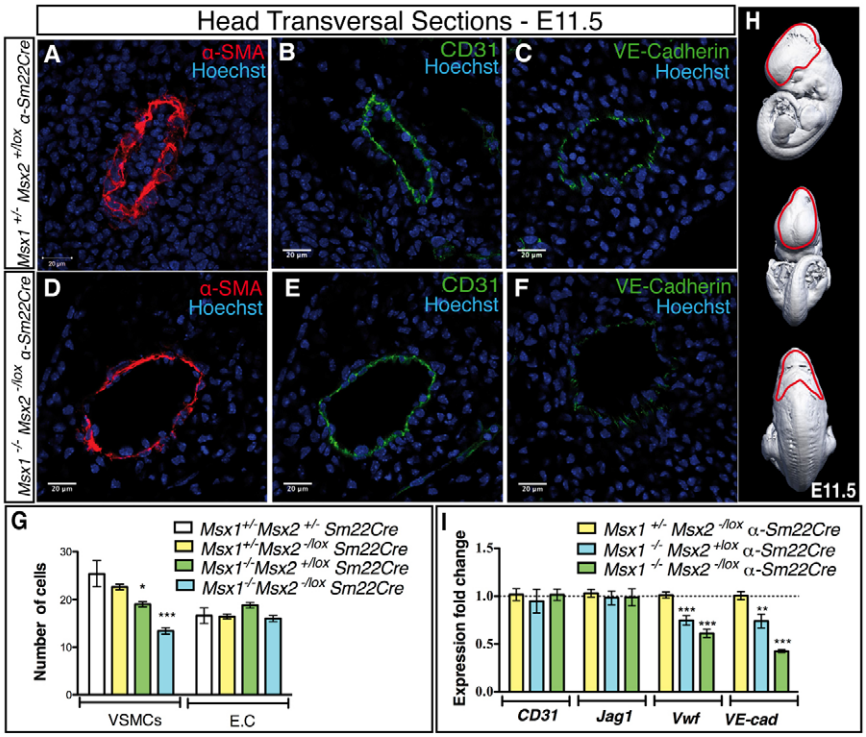

Fig. 2. Msx genes are crucial for proper VSMC coverage and endothelial maturation. (**A-F**) Immunofluorescence analyses of transverse sections from E11.5 mouse embryos show a strong decrease in the number of α-SMA-positive cells around the CA in the *Sm22Cre Msx1/2* mutant (D) as compared with the control (A). A reduction in the number of cells positive for VE-cad (F), but not CD31 (E), is also observed in mutants compared with controls (C and B, respectively). (**G**) The number of nuclei surrounded by α-SMA or CD31 was quantified in different genotypes. For each, *n*=5. (**H**,**I**) Reduction in expression of late-expressed endothelial genes was confirmed by qRT-PCR (I) using RNA from cephalic tissues dissected as described in H (red-outlined area). Expression of *Vwf* and *VE-cad* was reduced in the *Msx1* mutant and even further in the *Sm22Cre Msx1/2* mutant. By contrast, *Jag1* and *Cd31* showed no significant change. *, *P*<0.05; **, *P*<0.01; ***, *P*<0.001 (non-parametric Dunnett test). Error bars indicate s.e.m. Scale bars: 20 μm.

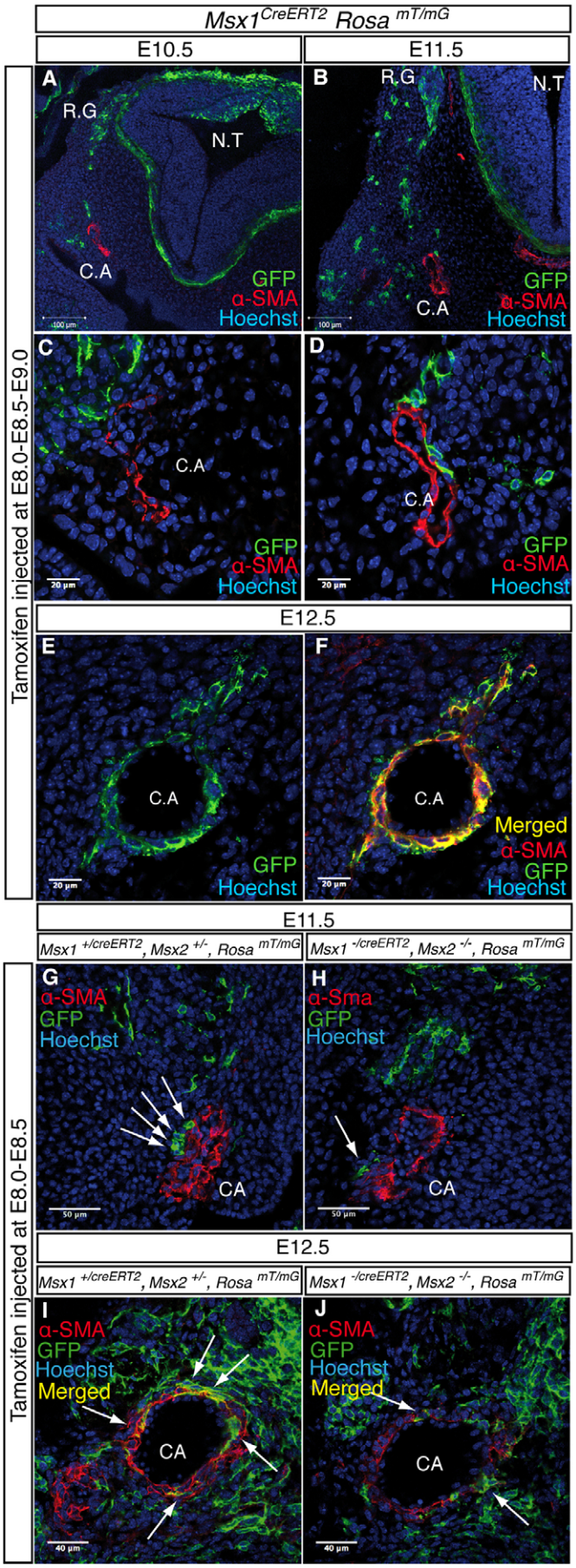

Fig. 3. *Msx1* and *Msx2* are essential in VSMC precursors. (**A-F**) Transverse sections of the head at E10.5 (A,C), E11.5 (B,D) and E12.5 (E,F). *Msx1*^{CreERT2} *Rosa*$^{mT/mG}$ gravid mice were injected with Tamoxifen at E8.0-E9.0. Cells expressing Cre-activated GFP are green, whereas α-SMA is red. (A,B) Low-magnification images reveal GFP-positive mesenchymal cells between the dorsal root ganglion (R.G) and the CA, suggesting a migration route for neural crest cells to the CA. (C-F) On higher magnification images, no GFP-positive cells can be detected in the mural layer of the CA at E10.5 (C). At E11.5 (D), some GFP-expressing cells are conspicuous close to the artery. At E12.5, many more GFP-positive cells are present in the mural layer (E), and most of them have started co-expressing α-SMA (F, yellow). N.T, neural tube. (**G-J**) Similar analysis on Msx double-heterozygous (G,I) or double-null (H,J) embryos matched from the same litters. Tamoxifen was injected at E8.0 and E8.5. In *Msx1*$^{-/-}$; *Msx2*$^{-/-}$ double-mutant embryos at E11.5 (H) and E12.5 (J), the global number of GFP-positive cells does not appear reduced as compared with controls (G and I, respectively). However, the number of GFP-positive cells reaching the artery and expressing α-SMA is significantly lower in the mutant (arrows). Scale bars: 100 μm in A,B; 50 μm in G,H; 40 μm in I,J; 20 μm in C-F.

expression level of a set of genes measured by qRT-PCR. In the *Sm22Cre Msx1/2* mutant, VSMC-specific transcripts were decreased in proportion to the reduced coverage of the vessels (see Fig. S3 in the supplementary material). The number of ECs was not reduced (Fig. 2G), and, accordingly, expression of *Cd31* (*Pecam1* – Mouse Genome Informatics) and jagged 1 (*Jag1*), two genes that are expressed early in the endothelium, was not affected by the mutation (Fig. 2B,E,I). Unexpectedly, the VE-cadherin (VE-cad; cadherin 5 – Mouse Genome Informatics) level appeared markedly decreased on sections (Fig. 2C,F). According to qRT-PCR (Fig. 2I), *VE-cad* transcripts were reduced by 26% in the *Msx1* single mutant and by 57% in the *Sm22Cre Msx1/2* double mutant. Similarly, von Willebrand factor (*Vwf*) transcripts were reduced by 25% and 39%, respectively. *VE-cad* and *Vwf* are among the genes that are expressed late in the endothelium (Dejana et al., 1989; Navarro et al., 1995), suggesting an impairment in maturation. The basal lamina, analyzed using collagen IV, laminin 1 and fibronectin antibodies, appeared normal in the *Sm22Cre Msx1/2* mutant (see Fig. S4 in the supplementary material).

At birth, vascular anomalies were observed in the head of *Sm22Cre Msx1/2* mutants. The superficial temporal artery showed more branching than in the control; aneurysms and hemorrhages were frequently observed (see Fig. S5 in the supplementary material). No major branching defect or hemorrhage was observed in either *Msx1* or *Sm22Cre Msx2*$^{lox/-}$ single mutants.

To identify the cell layer in which *Msx1* is required, we took advantage of a conditional allele (Fu et al., 2007) to selectively inactivate *Msx1* in the endothelium and in the VSMC lineages (see Fig. S6 in the supplementary material). This showed that *Sm22Cre*-driven inactivation of *Msx1* and *Msx2* results in the same phenotype as the *Sm22Cre Msx1/2* mutation, i.e. an increase in the CA section surface and a reduction in VSMC coverage (see Fig. S6A,B,D in the supplementary material). By contrast, *Tie2-Cre*-driven *Msx1* and *Msx2* inactivation did not affect the CA diameter or VSMC coverage (see Fig. S6B,C,D in the supplementary material). Therefore, *Msx1* is required in cells of the smooth muscle lineage, whereas there is no evidence for a role for Msx genes in the endothelium.

Msx1 and *Msx2* are expressed in VSMC progenitors

According to our results, the Msx1 and Msx2 transcription factors are essential for proper formation of the mural cell layer. However, the weak expression of $Msx1^{lacZ}$ in this layer precludes a role for Msx1 in mature VSMCs. An alternative explanation is that Msx genes are required in VSMC precursors before they are recruited to the vessel wall. To investigate this hypothesis, we constructed a Tamoxifen-inducible $Msx1^{CreERT2}$ allele (Y.L., J. Moreau, C.S.C., F. Langa-Vives and B.R., unpublished). Properties of this allele are briefly reported in Fig. S7 in the supplementary material. $Msx1^{CreERT2}$ was used in conjunction with the $Rosa^{mT/mG}$ allele (Muzumdar et al., 2007).

Pregnant dams were injected three times with Tamoxifen, at E8.0, E8.5 and E9.0, and the embryos analyzed at E10.5, E11.5 or E12.5. At E10.5 and E11.5, we observed a number of GFP-positive mesenchymal cells in the region between the neural crest-derived root ganglion and the CA (Fig. 3A,B). Furthermore, from E10.5 to E12.5, the VSMC layer was progressively populated by GFP-positive cells. Many of them co-expressed α-*Sma*, demonstrating that they had differentiated into bona fide VSMCs (Fig. 3C-F). The CA is just forming at E9.0 (Walls et al., 2008) and is unlikely to be covered by mural cells. Therefore, the GFP-positive cells we observed in the mural layer at E12.5 after $Msx1^{CreERT2}$ activation at E8.0-E9.0 are unlikely to derive from pre-existing mural cells proliferating in situ.

Using $Msx1^{CreERT2}$; $Rosa^{mT/mG}$, we further analyzed the covering of blood vessels by GFP-positive cells in an Msx null context, taking advantage of the fact that $Msx1^{CreERT2}$ is an *Msx1* null allele (Fig. 3G-J). Tamoxifen was injected at E8.0 and E8.5 and embryos analyzed at E11.5 or E12.5. At E11.5, when at least one functional allele for *Msx1* and *Msx2* remained, we observed GFP-positive cells in close proximity to the CA and a population of GFP-positive cells that had reached the mural layer (Fig. 3G, arrows). When both *Msx1* and *Msx2* were inactivated, GFP-positive cells similarly migrated to the CA region, but very few were found close to, or in, the mural layer (Fig. 3H, arrow), to which they failed to attach. At E12.5, significantly fewer GFP-positive cells were observed immediately adjacent to the CA and even fewer in the mural layer, in the mutant versus control (Fig. 3I,J).

Msx1-positive precursors were also observed to express $Msx2^{lacZ}$ before they integrated into the mural layer (see Fig. S8A in the supplementary material). Furthermore, we used the $Msx1^{CreERT2}$ allele to inactivate *Msx2* in an *Msx1* mutant context ($Msx1^{CreERT2/-}$; $Msx2^{lox/lox}$). Tamoxifen was injected at E8.0, E8.5 and E9.0. At E11.5, the CA exhibited the same abnormal phenotype as in *Sm22Cre Msx1/2* mutants, i.e. an increase in vessel diameter and the depletion of mural cells (see Fig. S8B,C in the supplementary material). We conclude that *Msx2* was inactivated by $Msx1^{CreERT2}$ in *Msx1*-expressing precursors before they reached the mural layer.

Msx genes are essential for proper *Mmp2* and *Mmp9* expression

The migration, survival and proliferation of VSMCs have been shown to depend on the matrix metalloproteinases Mmp2 and Mmp9 (reviewed by Newby, 2006). We therefore evaluated the level of Mmp2 protein by immunofluorescence on transverse sections of E12.5 embryos, in which *Msx1*-expressing precursors had been labeled with GFP at E8.0-E9.0 using $Msx1^{CreERT2}$ and $Rosa^{mT/mG}$ alleles (Fig. 4A-F). In the control, many GFP-positive cells accumulated Mmp2 and integrated in the mural layer, whereas very few cells did so in the mutant (compare Fig. 4A,C,E with 4B,D,F). Mmp reduction in the mutant was confirmed by qRT-PCR on cephalic VSMCs, which were FACS sorted from E12.5 embryo heads using the *Sm22α-Cre* transgene together with $Rosa^{mT/mG}$ (see Fig. S9 in the supplementary material). In $Msx1^{-/-}$; $Msx2^{-/-}$ mutant VSMCs, we observed a severe reduction in the expression of both

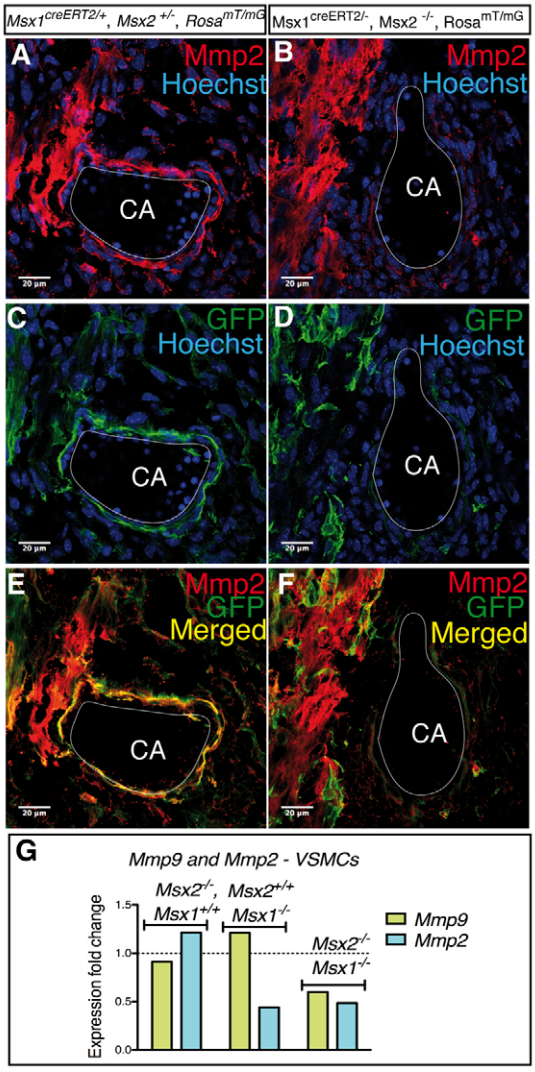

Fig. 4. Migration is altered in the Msx double mutants. (**A-F**) Head transverse sections of (A,C,E) $Msx1^{+/-}$; $Msx2^{+/-}$ double-heterozygous and (B,D,F) stage-matched $Msx1^{-/-}$; $Msx2^{-/-}$ double-homozygous mutant mouse embryos at E12.5. Early *Msx1*-expressing cells were labeled by GFP (green) at E8.0 and E8.5 using the $Msx1^{creERT2}$ allele, activated by Tamoxifen, together with the $Rosa^{mT/mG}$ reporter allele. In an $Msx1^{+/-}$; $Msx2^{+/-}$ context, we observe cells expressing Mmp2 (red) (A) and GFP (green) (C) in the CA mural layer as well as in surrounding regions. Overlap of the two labels (yellow) is extensive (E). In the $Msx1^{-/-}$; $Msx2^{-/-}$ mutant, the Mmp2 protein level is dramatically reduced in the CA mural layer, although the number of GFP-positive or Mmp2-positive cells outside the CA does not appear to be changed. (**G**) *Mmp2* and *Mmp9* expression levels were measured on FACS-sorted VSMCs by qRT-PCR. In the single *Msx1* mutant, *Mmp2* shows a severe decrease in expression that is in part balanced by overexpression of *Mmp9*. In the $Msx1^{-/-}$; $Msx2^{-/-}$ double mutant, a severe decrease in expression of both *Mmp2* and *Mmp9* is observed. Fold changes are relative to the level of expression in the $Msx1^{+/-}$; $Msx2^{+/-}$ double heterozygotes (dotted line). Scale bars: 20 μm.

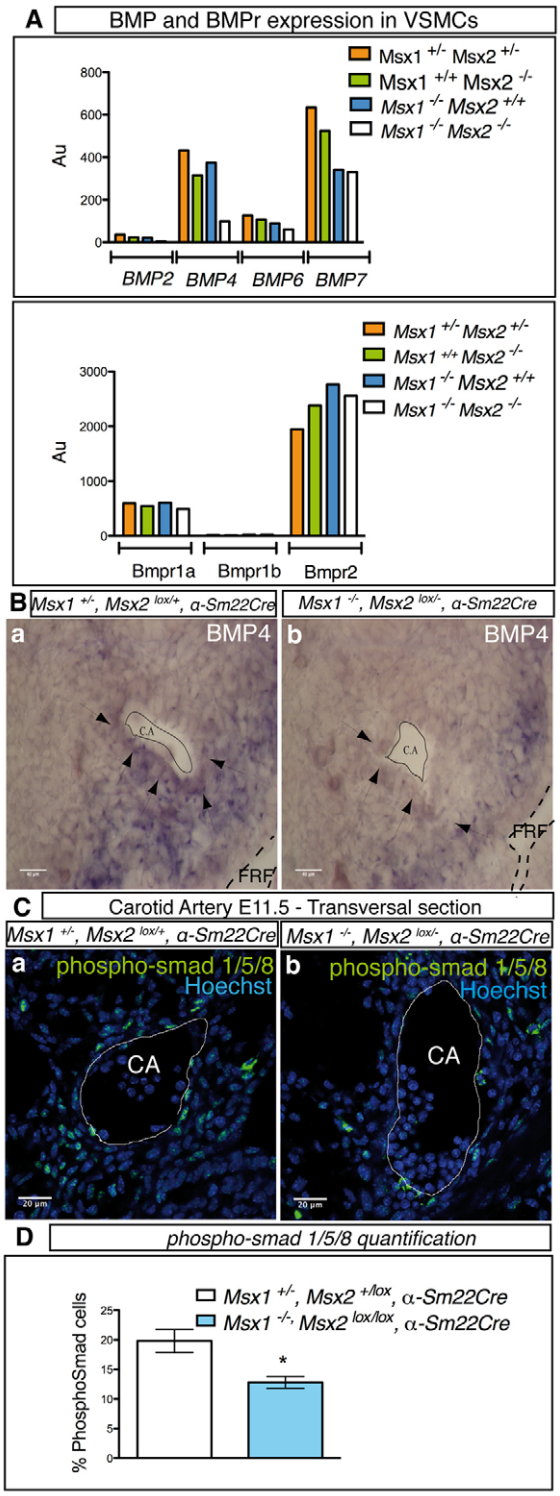

Fig. 5. Mmp2 and Mmp9 reduction is due to impairment in BMP signaling. (**A**) qRT-PCR analysis of FACS-sorted VSMCs. *Bmp4* expression decreases dramatically in *Msx1*$^{-/-}$; *Msx2*$^{-/-}$ mutant cells as compared with *Msx1*$^{+/-}$; *Msx2*$^{+/-}$ control cells. *Bmp7* is the most highly expressed BMP gene in the control cell population and its expression is reduced by 45% in the double-homozygous mutant. *Bmp2* and *Bmp6* are weakly expressed in control cells and almost undetectable in *Msx1*$^{-/-}$; *Msx2*$^{-/-}$ mutant cells. *Bmpr1a* and *Bmpr2* are highly expressed in the VSMCs at E12.5. Their expression is not significantly affected in *Msx1*$^{-/-}$; *Msx2*$^{-/-}$ cells. Au, arbitrary units. (**B**) In situ hybridization of head transverse sections of E11.5 embryos shows *Bmp4* mRNA accumulation mainly in and around the mural layer of the CA (**a**, arrowheads). No significant *Bmp4* expression was observed in the endothelium. In the double Msx mutant, the level of *Bmp4* mRNA is strongly reduced in cells of the mural layer and in close vicinity to the CA (**b**, arrowheads). By contrast, *Bmp4* expression remains elevated close to the pharyngeal region of the foregut (PRF). (**C**) To confirm the role of Msx genes in the BMP pathway, we performed an immunofluorescence assay for the phosphorylated forms of Smad1/5/8. In the double *Sm22Cre Msx1/2* mutant (**b**), there is a reduction in the number of phospho-Smad-positive cells relative to the control (**a**). (**D**) This reduction was quantified as the ratio between the number of phospho-Smad-labeled nuclei and the total number of Hoechst-positive nuclei. For both mutant and control, n=5. *, P<0.05 (non-parametric Dunnett test). Error bars indicate s.e.m. Scale bars: 40 μm in B; 20 μm in C.

Mmp2 (52% of control) and *Mmp9* (40%) (Fig. 4G). *Mmp2* expression was also reduced in the *Msx1*$^{-/-}$ mutant (56% of control), although in this genotype this was compensated by an increase in *Mmp9*. No reduction in Mmp expression was observed in the *Msx2*$^{-/-}$ mutant.

Mmp2 and Mmp9 are crucial for the survival and proliferation of VSMCs (Newby, 2006). However, we observed no change in apoptosis, using Lysotracker staining (see Fig. S10A,B in the supplementary material), or in proliferation rate, using an anti-phospho-histone H3 antibody (see Fig. S10C,D in the supplementary material), between controls and *Sm22Cre Msx1/2* mutants. Phospho-histone H3-positive cells represented 2.7% of the total cells in either genotype (see Fig. S10E in the supplementary material).

The BMP pathway is affected in *Msx1*$^{-/-}$; *Msx2*$^{-/-}$ VSMCs

Mmp2 and *Mmp9* have previously been characterized as targets of the BMP signaling pathway in mural cells (El-Bizri et al., 2008). Msx genes are involved in BMP signaling at several sites during development. We therefore analyzed the expression levels of a number of BMP ligands and receptors in VSMCs, FACS sorted as previously described (Fig. 5A). *Bmp4* showed the most significant downregulation in *Sm22Cre Msx1/2* mutant cells. *Bmp2*, *Bmp6* and *Bmp7* transcripts were also reduced, albeit to a lesser extent. The *Bmp2* expression level proved to be low and its variation is not expected to account for a reduction in overall BMP signaling. By contrast, *Bmp7* is expressed at a higher level than *Bmp4* and might contribute to this reduction in the mutant. No significant change in expression was observed for the BMP receptor genes *Bmpr1a*, *Bmpr1b* and *Bmpr2*.

The reduction of *Bmp4* expression around the CA was confirmed by in situ hybridization on sections from E11.5 *Sm22Cre Msx1/2* embryos (Fig. 5Bb). The reduction in BMP signaling was further demonstrated by analyzing Smad1/5/8 phosphorylation by immunohistochemistry at E11.5. The number of phospho-Smad-positive cells was conspicuously reduced in the double mutant (Fig. 5Cb). Quantification of phospho-Smad-positive cells on sections showed that 22% of the cells were stained with the anti-phospho-Smad antibody in control embryos versus 13% in the double mutant, corresponding to a 40% decrease (Fig. 5D).

To further demonstrate that, in the VSMC lineage, Msx genes act upstream of BMPs, VSMCs possessing one active allele of *Msx1* and *Msx2* were sorted using *Sm22α*-activated *Rosa*$^{mT/mG}$, and

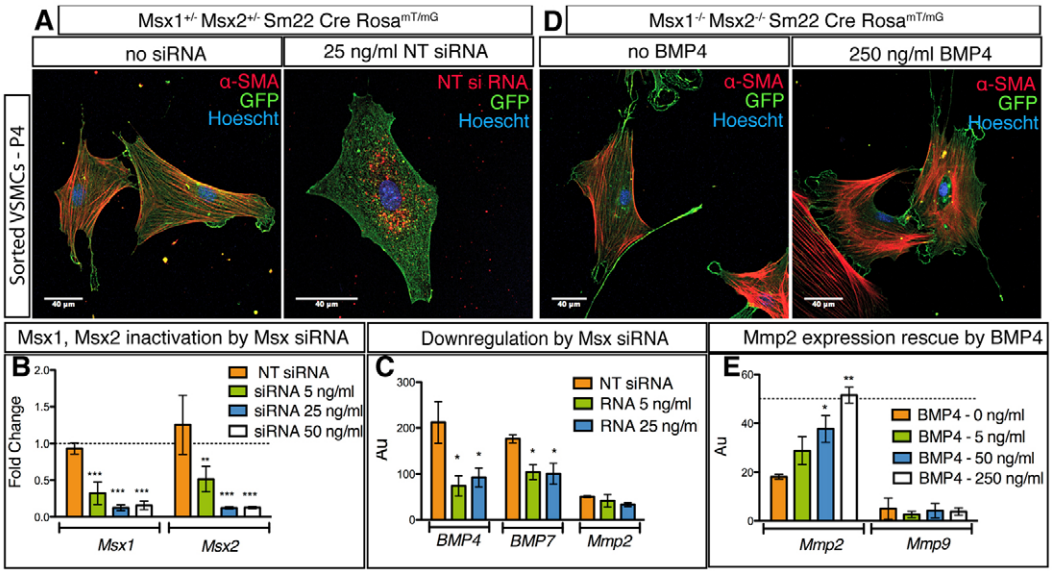

Fig. 6. Ex vivo analyses confirm that *Bmp4* is downstream of Msx genes in VSMCs. (**A-E**) After four passages, FACS-sorted VSMCs maintain α-SMA expression (red) and smooth muscle cell morphology (A,D). Non-targeted (NT) fluorescent siRNA was transfected successfully and is localized in the cell cytoplasm (A). *Msx1*$^{+/-}$; *Msx2*$^{+/-}$ cells were transfected with increasing concentrations of *Msx1* plus *Msx2* siRNAs (B,C). Maximal (88%) inactivation of *Msx1* and *Msx2* was reached using 25 ng/ml of siRNA (B). Downregulation of Msx gene expression had a significant impact on *Bmp4* and *Bmp7* expression (57% and 43%, respectively) and a lesser impact on *Mmp2* (35%) (C). To confirm an effect of Bmp4 on *Mmp2* and *Mmp9* expression, we added increasing amounts of exogenous Bmp4 to *Msx1*$^{-/-}$; *Msx2*$^{-/-}$ VSMCs (D,E). This did not affect cell viability or phenotype (D). *Mmp2* expression increases proportionally with Bmp4 concentration (E). The *Mmp2* endogenous expression level in *Msx1*$^{+/-}$; *Msx2*$^{+/-}$ cells is represented by the dotted horizontal line. *Mmp9* expression in cultured VSMCs decreased to insignificant levels and, consequently, no conclusion could be drawn for this gene. *, $P<0.05$; **, $P<0.01$; ***, $P<0.001$ (non-parametric Dunnett test). Error bars indicate s.e.m. Scale bars: 40 μm.

Msx gene inactivation was mimicked in culture using Msx-targeted siRNAs. VSMCs retained their phenotype when cultured, based on α-*Sma* expression and morphological characteristics (Fig. 6A). Transfection efficiency was assessed using a fluorescent non-targeted siRNA (NT siRNA) (Fig. 6A), which did not interfere with *Msx1* or *Msx2* expression (Fig. 6B). Increasing amounts of Msx-specific siRNAs progressively reduced *Msx1* and *Msx2* transcript levels, reaching maximal efficiency at 25 ng/ml (Fig. 6B). Under these conditions, 88% of *Msx1* and *Msx2* transcripts were lost. *Bmp4* and *Bmp7* transcripts were correspondingly reduced, as were those of *Mmp2* (Fig. 6C). To obtain further confirmation, VSMC precursors were sorted in the same way from *Msx1; Msx2* double-null mutants and, after a few days in culture, they were demonstrated to express low levels of *Mmp2* and insignificant levels of *Mmp9* transcripts. After 48 hours in culture with increasing amounts of exogenous Bmp4, the cells did not show phenotypic changes (Fig. 6D) but the *Mmp2* expression levels were raised significantly and in a dose-dependent manner (Fig. 6E).

Altogether, these results confirm that Msx genes act upstream of *Bmp4* and *Bmp7* in VSMC progenitors and that, as previously demonstrated (El Bizri et al., 2008), BMP signaling is required for *Mmp2* expression. In culture, *Mmp9* expression decreases dramatically and so no conclusion could be drawn for this gene.

Reduced VSMC coverage leads to a reduction in mural-to-endothelial cell signaling and impairs endothelium maturation

As mentioned above, whereas the number of ECs and the expression of early endothelial markers were not decreased in the *Sm22Cre Msx1/2* mutant, late-expressed endothelial markers were downregulated (Fig. 2G). We verified that this did not correlate with a change in arteriovenous identity of the CA using antibodies against neuropilin 1, an artery-specific marker (Klagsbrun et al., 2002) (see Fig. S11 in the supplementary material). Downregulation of endothelial markers suggested that reduced VSMC coverage leads to impairment in signaling between the two layers, resulting in defects in endothelium maturation. By qRT-PCR, we did not observe a significant difference in the expression of ligands produced by the endothelium, such as *Tgfb1* or *Pdgfb*, in single or double Msx mutants as compared with controls (Fig. 7A). By contrast, mRNAs for mural cell-secreted factors were detected at lower levels in the *Sm22Cre Msx1/2* mutants. *Vegfa* and *Angpt1* levels were decreased by 37% and 36%, respectively (Fig. 7B). This can be readily explained by the reduction in mural cell coverage, which would impact on the endothelium. It has recently been demonstrated in culture that Tie2 (Tek – Mouse Genome Informatics) is concentrated at the cell membrane by its ligand Angpt1 (Fukuhara et al., 2008; Saharinen et al., 2008). In keeping with these results, we observed in normal embryos a high concentration of Tie2 at the EC membrane on the external side, facing the mural cells, and on the lateral side adjacent to neighboring ECs (Fig. 7C,C′,D). By contrast, Tie2 was diffusely distributed over the EC membrane in the *Sm22Cre Msx1/2* mutant (Fig. 7E,E′,F), correlating with the decreased Angpt1 secretion by the thinner mural layer.

To confirm these results, we sorted ECs by FACS (using a CD31 antibody) from E12.5 heads (see Fig. S9 in the supplementary material). In ECs, Kruppel-like factor 2 (*Klf2*) expression is dependent on Tie2 activation (Sako et al., 2009). Accordingly, we detected a 50% decrease in *Klf2* expression in the constitutive *Msx1; Msx2* double-mutant ECs (Fig. 7G). Fig. 7H summarizes the consequences for the endothelium of the reduction in mural cell coverage associated with Msx deficiency.

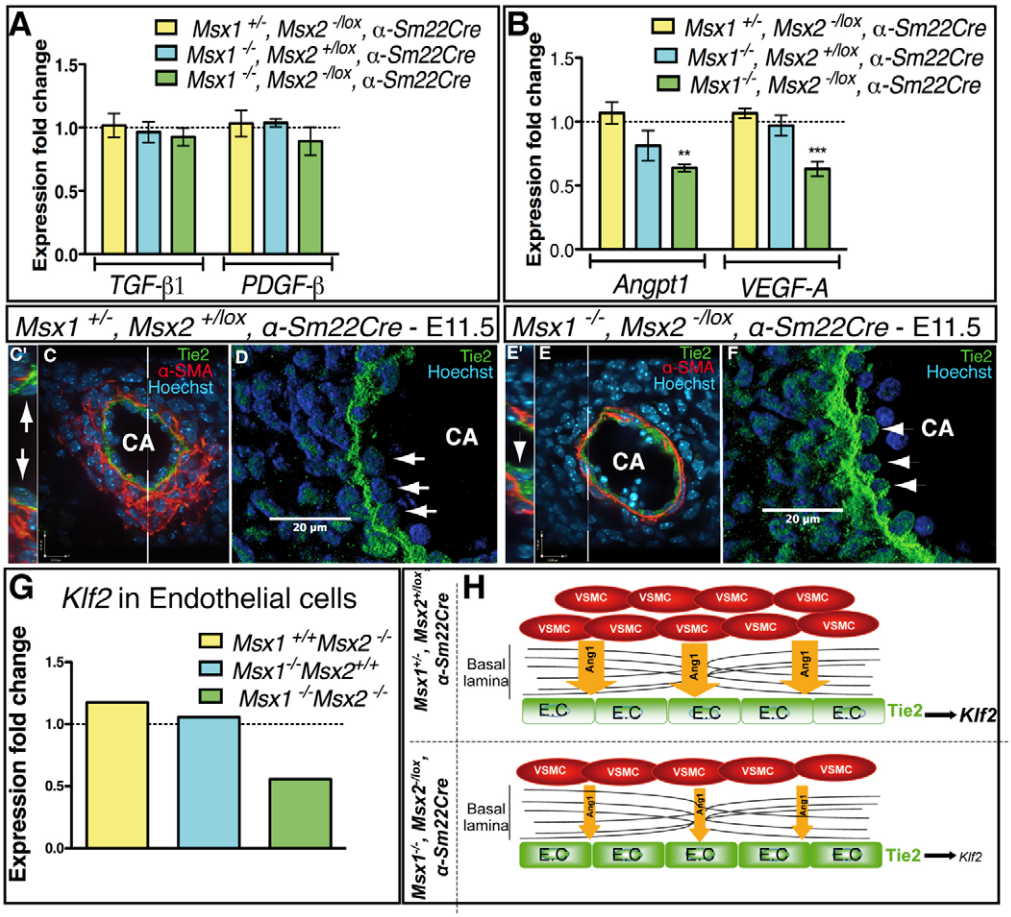

Fig. 7. Improper VSMC coverage leads to impairment of endothelium maturation. (**A**) qRT-PCR of cephalic tissue RNA (see Fig. 2H) shows no significant decrease in the level of endothelial-to-mural signaling factors, such as *Pdgfb* and *Tgfb1*, in the *Sm22Cre Msx1/2* mutant. (**B**) By contrast, expression of *Angpt1* and *Vegfa*, two genes associated with mural-to-endothelial cell communication, is significantly decreased in the mutant. **, $P<0.01$; ***, $P<0.001$ (non-parametric Dunnett test). (**C-F**) Transverse sections of carotid arteries from E11.5 control (C,C′) or *Sm22Cre Msx1/2* mutant (E,E′) embryos were labeled for Tie2 (green) and α-SMA (red). Nuclear Hoechst is in blue. Tie2 in the endothelium appears localized close to the VSMC layer (α-SMA positive) in normal (C,C′,D), but more diffuse over the whole EC membrane in mutant (E,E′,F) embryo vessels. This is more conspicuous in higher magnifications images (D,F). Arrows point to endothelial nuclei that are on the luminal side of the artery relative to Tie2 protein in the control (C′,D); arrowheads point to endothelial nuclei that appear embedded in the Tie2 expression domain in the mutant (E′,F). This is further exemplified in optical stacks along the *z*-axis of the same sections (C′,E′). Optical section planes for C′ and E′ are shown in C and E, respectively (thin lines). (**G**) qRT-PCR analysis of FACS-sorted CD31-positive cells shows that *Klf2* expression is reduced in the *Msx1*$^{-/-}$*; Msx2*$^{-/-}$ mutant as compared with either single *Msx1*$^{-/-}$ or *Msx2*$^{-/-}$ mutant. Changes in expression are expressed as fold changes relative to control (dotted line). (**H**) Schematic interpretation of the results. VSMCs are represented in red, secreted Angpt1 (Ang1) protein in yellow, Tie2 receptor in green and Klf2 protein in black. Reduction in VSMCs leads to lower Angpt1 secretion, which results in a reduced concentration of Tie2 at the mural side of the EC membrane and in a reduction in *Klf2* expression. Error bars indicate s.e.m. Scale bars: 20 µm.

DISCUSSION

An essential role for Msx genes in the head vasculature

We report for the first time that combined *Msx1* and *Msx2* gene deficiencies lead to major defects in blood vessels: an excess of branching and increase in caliber of major head arteries such as the CA, hemorrhages and aneurysms. None of these defects is observed in *Msx1* or *Msx2* single mutants. These vascular defects are related to a reduction in the mural cell coverage of head arteries.

Similar to the cardiac outflow tract (Rentschler et al., 2010), VSMCs in most head vessels derive from neural crest cells (NCCs), whereas the endothelium is of mesodermal origin (Jiang et al., 2000; Etchevers et al., 2001; Korn et al., 2002). In particular, in the mouse embryo, the contribution of NCCs has been demonstrated for the CAs, whereas neural crest-derived VSMCs could not be detected at any stage in the dorsal aorta (Jiang et al., 2000), for which VSMCs have been shown to share a lineage with somitic mesoderm (Esner et al., 2006; Wiegreffe et al., 2009). *Msx1* and *Msx2* are strongly expressed in NCCs (for reviews, see Bendall and Abate-Shen, 2000; Ramos and Robert, 2005). Unlike *Xenopus*, in which *Msx1* is mandatory for neural crest formation (Monsoro-Burq et al., 2005), combined deficiencies of *Msx1* and *Msx2* do not preclude neural crest formation or migration in the mouse. However, they severely affect neural crest subpopulations, resulting in pleiotropic defects in NCC derivatives (Ishii et al., 2005). Thus, the *Msx1; Msx2* double mutation impairs the differentiation, but not migration, of cranial NCCs that form the frontal bones (Han et al., 2007). In the outflow tract of the heart, Msx genes are required to inhibit excessive proliferation of post-migratory NCCs (Chen et al.,

2007). By contrast, Msx genes do not seem to play a role in the proliferation of the neural crest-derived cells that contribute to the cranial ganglia and the first pharyngeal arch, but instead function in preventing their apoptosis (Ishii et al., 2005).

We propose that the head smooth muscle defects reported here are linked to a specific neural crest subpopulation that depends on functional Msx genes to give rise to smooth muscle progenitor cells. Indeed, some images (Fig. 3A,B) strongly suggest that the *Msx1*-expressing VSMC precursors migrate from dorsal regions. Of note, some VSMCs form in Msx mutant head vessels, confirming that only a subpopulation of precursors is affected. This is in agreement with the heterogeneity of origin of VSMCs (reviewed by Majesky, 2007). In addition, we have not observed branching defects in the intersomitic vessels or a reduction in the mural coverage of the dorsal aorta (data not shown). Thus, Msx deficiency does not seem to affect non-neural crest-derived VSMCs or the vessels that they cover.

Msx1 is expressed in VSMC precursors that require Msx genes to migrate to the CA

At E12.5, *Msx1* is predominantly expressed in the endothelium. Defects in the double mutant might therefore result from the conjunction of *Msx1* deficiency in the endothelium and *Msx2* deficiency in the VSMCs. However, the same abnormal vascular phenotype was observed in *Sm22α-Cre; Msx1*$^{lox/lox}$*; Msx2*$^{lox/lox}$ mutants, whereas the specific mutation of *Msx1* and *Msx2* in the endothelium did not lead to vascular defects. Our data show that the primary defect in the *Sm22Cre Msx1/2* mutant lies in mural cell precursors before they reach the blood vessels. The *Sm22Cre* transgene that we used is expressed early in the mural lineage (see Fig. S2 in the supplementary material), allowing inactivation of *Msx1* and *Msx2* before VSMCs attach to the mural layer. Taking advantage of the *Msx1*^{CreERT2} allele and an inducible reporter, we could trace back cells that once expressed *Msx1*. Tamoxifen injections were performed at stages (E8.0-E9.0) when mural cells have not yet differentiated in the head vessels (Walls et al., 2008). Under these conditions, many GFP-positive cells were observed at E11.5 and even more at E12.5 in the mural layer. This implies that these cells derive from VSMC precursors that express *Msx1*, which migrate to progressively populate the mural layer. VSMCs derived from *Msx1*-expressing precursors no longer express *Msx1* after differentiation. Similarly, switch-off of *Msx1* expression before differentiation has been reported for VSMC adventitial progenitors in the aorta (Passman et al., 2008).

Cell lineage studies clearly demonstrate that cells derived from *Msx1*-expressing precursors accumulate in normal amounts in the region around the CA, in a context of Msx deficiency. However, most of these cells fail to reach the artery and to integrate into the mural layer. This suggests late migration defects in the VSMC precursors, linked to the reduction in *Mmp2* and *Mmp9* expression in the mutant. Mmp2 and Mmp9 are known to free smooth muscle cells from the cell-matrix contacts that normally restrict their migration (Kenagy et al., 1997; Newby, 2006). The majority of *Msx1*-expressing VSMC precursors that fail to reach the CA do not accumulate detectable amounts of Mmp2 and might therefore be impeded in making their way through the vessel ECM. Of note, some cells manage to integrate into the mural layer even though they do not express Mmp2. These cells possibly express other proteinases, in keeping with the phenotypic heterogeneity of VSMCs (Majesky, 2007).

Proper BMP signaling in head VSMCs depends on Msx genes

Msx genes have been previously associated with BMP signaling at several sites during development. Functional analysis of tooth or palate formation further demonstrated that these genes can act either upstream or downstream of *Bmp4* (Chen et al., 1996; Zhang et al., 2002). *Sm22Cre Msx1/2* double mutants exhibit a severe downregulation of the BMP pathway in the VSMC lineage. Bmp7 is the prevalent ligand of this family in the head VSMCs and its depletion, together with that of Bmp4, should result in a strong reduction in global BMP signaling in mutant VSMCs. The BMP pathway has pleiotropic effects on the vasculature, as discussed by Abe (Abe, 2006). Manipulations that reduce BMP levels usually result in impairment of VSMC coverage and in a correlative dilation of the vessel, e.g. *Flk1*-driven deletion of *Bmpr1a* (Park et al., 2006), *Sm22α*-driven deletion of *Bmpr1a* (El-Bizri et al., 2008), knockdown of *Bmpr2* (Liu et al., 2007) and mutation of *Smad5* (Yang et al., 1999). These phenotypes are strikingly similar to those we describe in the head vessels of the *Sm22Cre Msx1/2* mutant.

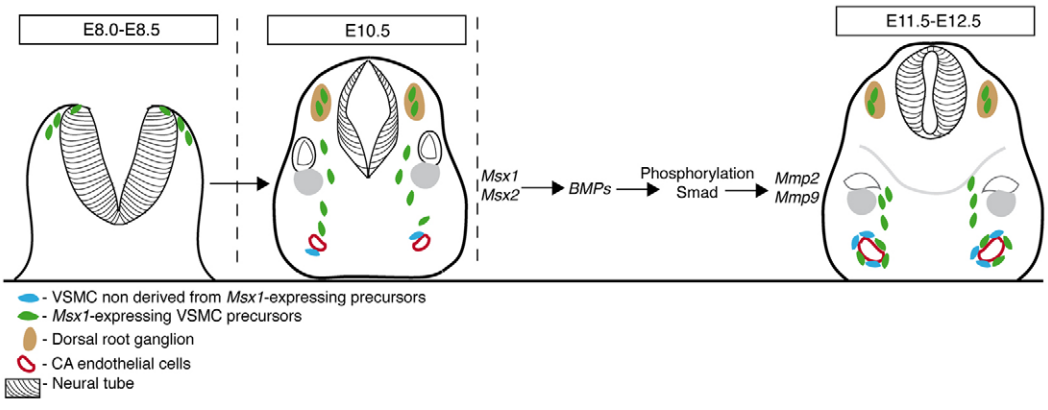

Fig. 8. The role of Msx genes in a subpopulation of VSMCs. Using the *Msx1*^{CreERT2} and the *Rosa*$^{mT/mG}$ alleles, we labeled *Msx1*-expressing cells at E8.0-E8.5. At this stage, Msx1 is strongly expressed in the neural crest, from which head VSMCs originate. At E10.5, we observed GFP-positive cells close to the CA but not in contact with it. Additionally, we observed a significant number of GFP-positive cells in the dorsal root ganglia and in the region between the latter and the CA. We have shown that Msx genes are essential for the late migration of a subpopulation of VSMC precursors via the control of BMP signaling and *Mmp2* and *Mmp9* expression. The expression of *Mmp2* and *Mmp9* correlates with the phosphorylation of Smad1/5/8.

Interestingly, the BMP pathway plays a major role in *Mmp2* and *Mmp9* expression. *Sm22α-Cre*-driven inactivation of *Bmpr1a* severely affects *Mmp2* and *Mmp9* expression in VSMCs, which leads to a reduction in mural cell coverage and consequent vessel dilation (El-Bizri et al., 2008). In head VSMCs, Msx genes seem to act upstream of BMP expression and consequently before BMP receptor activation, as the level of Smad phosphorylation is reduced in the double mutant. Indeed, we show that *Mmp2* expression can be rescued in mutant VSMCs by exogenous Bmp4. Furthermore, Roybal et al. (Roybal et al., 2010) have shown that *Bmp4* expression is similarly decreased in NCC-derived osteogenic cells upon inactivation of both *Msx1* and *Msx2* by a *Wnt1-Cre* transgene, although the overall level of BMP signaling is enhanced. Altogether, these results suggest an autocrine or paracrine mechanism among VSMCs producing their own BMPs. This is in keeping with the observation that gut smooth muscle precursor cells also produce BMPs and their receptors concurrently (Torihashi et al., 2009).

Impaired VSMC coverage indirectly affects the endothelium

In the *Sm22Cre Msx1/2* mutant, markers expressed late in the endothelium (*Vwf*, *VE-cad*) are downregulated. This suggests that impairment of the endothelium maturation process derives from defects in mural cells. Indeed, reduction in the *Angpt1* expression level correlates well with the reduction in the number of VSMCs, which predominantly secrete this factor. A decrease in *Angpt1* expression leads to a change in the membrane localization of Tie2 in ECs, as demonstrated in cell culture (Fukuhara et al., 2008; Saharinen et al., 2008) and which we confirm in vivo. Furthermore, the expression of *Klf2*, which is induced by activation of Angpt1 (De Val and Black, 2009; Sako et al., 2009), is significantly reduced in mutant ECs. Our interpretation is that reduced coverage by mural cells leads to a reduction in the secretion of mural factors, such as Angpt1. Consequently, there is an incomplete activation of endothelial receptors (such as Tie2), resulting in impairment of EC maturation.

Conclusion

Our in vivo data show that the Msx family of homeodomain transcription factors plays a major role in head vascular maturation and that their mutation leads to mural layer defects. We demonstrate *Msx1* expression in VSMC precursors, which require both *Msx1* and *Msx2* in order to integrate into the mural layer. We propose the following mechanism (Fig. 8): in head VSMCs, Msx factors act upstream of the BMP expression that controls the expression of *Mmp2* and *Mmp9*; deficiency in these metalloproteinases prevents VSMCs from reaching the mural layer, leading to reduced mural coverage, vessel dilation and impairment of endothelium maturation.

Acknowledgements

We are very grateful to Drs Margaret Buckingham, Colin Crist, Stéphane Vincent and Didier Montarras for critical reading of the manuscript, to Dr Robert Maxson and Dr Masashi Yanagisawa for generously sharing mouse strains, to Prof. Pierre Chambon for the gift of CreERT2, and to Pierre-Henri Commere from the flow cytometry platform of the Institut Pasteur for cell sorting. This work was supported by the Institut Pasteur, the CNRS and grants from the French Association pour la Recherche sur le Cancer (ARC) and Ligue contre le Cancer (LCC). M.L. is the recipient of a fellowship from the Portuguese Fundação Ciência e Tecnologia (FCT).

Competing interests statement

The authors declare no competing financial interests.

Supplementary material

Supplementary material for this article is available at
http://dev.biologists.org/lookup/suppl/doi:10.1242/dev.063214/-/DC1

References

Abe, J. (2006). Bone morphogenetic protein (BMP) family, SMAD signaling and Id helix-loop-helix proteins in the vasculature: the continuous mystery of BMPs pleotropic effects. *J. Mol. Cell. Cardiol.* **41**, 4-7.

Alappat, S., Zhang, Z. Y. and Chen, Y. P. (2003). Msx homeobox gene family and craniofacial development. *Cell Res.* **13**, 429-442.

Bach, A., Lallemand, Y., Nicola, M. A., Ramos, C., Mathis, L., Maufras, M. and Robert, B. (2003). Msx1 is required for dorsal diencephalon patterning. *Development* **130**, 4025-4036.

Bai, H., Gao, Y., Arzigian, M., Wojchowski, D. M., Wu, W. S. and Wang, Z. Z. (2010). BMP4 regulates vascular progenitor development in human embryonic stem cells through a smad-dependent pathway. *J. Cell. Biochem.* **109**, 363-374.

Battegay, E. J., Raines, E. W., Seifert, R. A., Bowen-Pope, D. F. and Ross, R. (1990). TGF-beta induces bimodal proliferation of connective tissue cells via complex control of an autocrine PDGF loop. *Cell* **63**, 515-524.

Bendall, A. J. and Abate-Shen, C. (2000). Roles for Msx and Dlx homeoproteins in vertebrate development. *Gene* **247**, 17-31.

Bensoussan, V., Lallemand, Y., Moreau, J., Cloment, C. S., Langa, F. and Robert, B. (2008). Generation of an Msx2-GFP conditional null allele. *Genesis* **46**, 276-282.

Chen, Y., Bei, M., Woo, I., Satokata, I. and Maas, R. (1996). Msx1 controls inductive signaling in mammalian tooth morphogenesis. *Development* **122**, 3035-3044.

Chen, Y. H., Ishii, M., Sun, J., Sucov, H. M. and Maxson, R. E., Jr (2007). Msx1 and Msx2 regulate survival of secondary heart field precursors and post-migratory proliferation of cardiac neural crest in the outflow tract. *Dev. Biol.* **308**, 421-437.

De Val, S. and Black, B. L. (2009). Transcriptional control of endothelial cell development. *Dev. Cell* **16**, 180-195.

Dejana, E., Lampugnani, M. G., Giorgi, M., Gaboli, M., Federici, A. B., Ruggeri, Z. M. and Marchisio, P. C. (1989). Von Willebrand factor promotes endothelial cell adhesion via an Arg-Gly-Asp-dependent mechanism. *J. Cell Biol.* **109**, 367-375.

El-Bizri, N., Guignabert, C., Wang, L., Cheng, A., Stankunas, K., Chang, C. P., Mishina, Y. and Rabinovitch, M. (2008). SM22alpha-targeted deletion of bone morphogenetic protein receptor 1A in mice impairs cardiac and vascular development, and influences organogenesis. *Development* **135**, 2981-2991.

Esner, M., Meilhac, S. M., Relaix, F., Nicolas, J. F., Cossu, G. and Buckingham, M. E. (2006). Smooth muscle of the dorsal aorta shares a common clonal origin with skeletal muscle of the myotome. *Development* **133**, 737-749.

Etchevers, H. C., Vincent, C., Le Douarin, N. M. and Couly, G. F. (2001). The cephalic neural crest provides pericytes and smooth muscle cells to all blood vessels of the face and forebrain. *Development* **128**, 1059-1068.

Feil, R., Brocard, J., Mascrez, B., LeMeur, M., Metzger, D. and Chambon, P. (1996). Ligand-activated site-specific recombination in mice. *Proc. Natl. Acad. Sci. USA* **93**, 10887-10890.

Finnerty, J. R., Mazza, M. E. and Jezewski, P. A. (2009). Domain duplication, divergence, and loss events in vertebrate Msx paralogs reveal phylogenomically informed disease markers. *BMC Evol. Biol.* **9**, 18.

Fu, H., Ishii, M., Gu, Y. and Maxson, R. (2007). Conditional alleles of Msx1 and Msx2. *Genesis* **45**, 477-481.

Fukuhara, S., Sako, K., Minami, T., Noda, K., Kim, H. Z., Kodama, T., Shibuya, M., Takakura, N., Koh, G. Y. and Mochizuki, N. (2008). Differential function of Tie2 at cell-cell contacts and cell-substratum contacts regulated by angiopoietin-1. *Nat. Cell Biol.* **10**, 513-526.

Goupille, O., Saint Cloment, C., Lopes, M., Montarras, D. and Robert, B. (2008). Msx1 and Msx2 are expressed in sub-populations of vascular smooth muscle cells. *Dev. Dyn.* **237**, 2187-2194.

Han, J., Ishii, M., Bringas, P., Jr, Maas, R. L., Maxson, R. E., Jr and Chai, Y. (2007). Concerted action of Msx1 and Msx2 in regulating cranial neural crest cell differentiation during frontal bone development. *Mech. Dev.* **124**, 729-745.

Hellstrom, M., Kalen, M., Lindahl, P., Abramsson, A. and Betsholtz, C. (1999). Role of PDGF-B and PDGFR-beta in recruitment of vascular smooth muscle cells and pericytes during embryonic blood vessel formation in the mouse. *Development* **126**, 3047-3055.

Houzelstein, D., Cohen, A., Buckingham, M. E. and Robert, B. (1997). Insertional mutation of the mouse Msx1 homeobox gene by an nlacZ reporter gene. *Mech. Dev.* **65**, 123-133.

Ishii, M., Han, J., Yen, H. Y., Sucov, H. M., Chai, Y. and Maxson, R. E., Jr (2005). Combined deficiencies of Msx1 and Msx2 cause impaired patterning and survival of the cranial neural crest. *Development* **132**, 4937-4950.

Jain, R. K. (2003). Molecular regulation of vessel maturation. *Nat. Med.* **9**, 685-693.

Jiang, X., Rowitch, D. H., Soriano, P., McMahon, A. P. and Sucov, H. M. (2000). Fate of the mammalian cardiac neural crest. *Development* **127**, 1607-1616.
Kapadia, H., Mues, G. and D'Souza, R. (2007). Genes affecting tooth morphogenesis. *Orthod. Craniofac. Res.* **10**, 105-113.
Kenagy, R. D., Hart, C. E., Stetler-Stevenson, W. G. and Clowes, A. W. (1997). Primate smooth muscle cell migration from aortic explants is mediated by endogenous platelet-derived growth factor and basic fibroblast growth factor acting through matrix metalloproteinases 2 and 9. *Circulation* **96**, 3555-3560.
Kisanuki, Y. Y., Hammer, R. E., Miyazaki, J., Williams, S. C., Richardson, J. A. and Yanagisawa, M. (2001). Tie2-Cre transgenic mice: a new model for endothelial cell-lineage analysis in vivo. *Dev. Biol.* **230**, 230-242.
Klagsbrun, M., Takashima, S. and Mamluk, R. (2002). The role of neuropilin in vascular and tumor biology. *Adv. Exp. Med. Biol.* **515**, 33-48.
Korn, J., Christ, B. and Kurz, H. (2002). Neuroectodermal origin of brain pericytes and vascular smooth muscle cells. *J. Comp. Neurol.* **442**, 78-88.
Lallemand, Y., Nicola, M. A., Ramos, C., Bach, A., Cloment, C. S. and Robert, B. (2005). Analysis of Msx1; Msx2 double mutants reveals multiple roles for Msx genes in limb development. *Development* **132**, 3003-3014.
Lallemand, Y., Bensoussan, V., Cloment, C. S. and Robert, B. (2009). Msx genes are important apoptosis effectors downstream of the Shh/Gli3 pathway in the limb. *Dev. Biol.* **331**, 189-198.
Liu, D., Wang, J., Kinzel, B., Mueller, M., Mao, X., Valdez, R., Liu, Y. and Li, E. (2007). Dosage-dependent requirement of BMP type II receptor for maintenance of vascular integrity. *Blood* **110**, 1502-1510.
Majack, R. A. (1987). Beta-type transforming growth factor specifies organizational behavior in vascular smooth muscle cell cultures. *J. Cell Biol.* **105**, 465-471.
Majesky, M. W. (2007). Developmental basis of vascular smooth muscle diversity. *Arterioscler. Thromb. Vasc. Biol.* **27**, 1248-1258.
Monsoro-Burq, A. H., Wang, E. and Harland, R. (2005). Msx1 and Pax3 cooperate to mediate FGF8 and WNT signals during Xenopus neural crest induction. *Dev. Cell* **8**, 167-178.
Muzumdar, M. D., Tasic, B., Miyamichi, K., Li, L. and Luo, L. (2007). A global double-fluorescent Cre reporter mouse. *Genesis* **45**, 593-605.
Navarro, P., Caveda, L., Breviario, F., Mandoteanu, I., Lampugnani, M. G. and Dejana, E. (1995). Catenin-dependent and -independent functions of vascular endothelial cadherin. *J. Biol. Chem.* **270**, 30965-30972.
Newby, A. C. (2006). Matrix metalloproteinases regulate migration, proliferation, and death of vascular smooth muscle cells by degrading matrix and non-matrix substrates. *Cardiovasc. Res.* **69**, 614-624.
Nishishita, T. and Lin, P. C. (2004). Angiopoietin 1, PDGF-B, and TGF-beta gene regulation in endothelial cell and smooth muscle cell interaction. *J. Cell. Biochem.* **91**, 584-593.
Park, C., Lavine, K., Mishina, Y., Deng, C. X., Ornitz, D. M. and Choi, K. (2006). Bone morphogenetic protein receptor 1A signaling is dispensable for hematopoietic development but essential for vessel and atrioventricular endocardial cushion formation. *Development* **133**, 3473-3484.
Passman, J. N., Dong, X. R., Wu, S. P., Maguire, C. T., Hogan, K. A., Bautch, V. L. and Majesky, M. W. (2008). A sonic hedgehog signaling domain in the arterial adventitia supports resident Sca1+ smooth muscle progenitor cells. *Proc. Natl. Acad. Sci. USA* **105**, 9349-9354.
Ramos, C. and Robert, B. (2005). msh/Msx gene family in neural development. *Trends Genet.* **21**, 624-632.
Rentschler, S., Jain, R. and Epstein, J. A. (2010). Tissue-tissue interactions during morphogenesis of the outflow tract. *Pediatr. Cardiol.* **31**, 408-413.
Risau, W. (1997). Mechanisms of angiogenesis. *Nature* **386**, 671-674.
Roybal, P. G., Wu, N. L., Sun, J., Ting, M. C., Schafer, C. A. and Maxson, R. E. (2010). Inactivation of Msx1 and Msx2 in neural crest reveals an unexpected role in suppressing heterotopic bone formation in the head. *Dev. Biol.* **343**, 28-39.
Saharinen, P., Eklund, L., Miettinen, J., Wirkkala, R., Anisimov, A., Winderlich, M., Nottebaum, A., Vestweber, D., Deutsch, U., Koh, G. Y. et al. (2008). Angiopoietins assemble distinct Tie2 signalling complexes in endothelial cell-cell and cell-matrix contacts. *Nat. Cell Biol.* **10**, 527-537.
Sako, K., Fukuhara, S., Minami, T., Hamakubo, T., Song, H., Kodama, T., Fukamizu, A., Gutkind, J. S., Koh, G. Y. and Mochizuki, N. (2009). Angiopoietin-1 induces Kruppel-like factor 2 expression through a phosphoinositide 3-kinase/AKT-dependent activation of myocyte enhancer factor 2. *J. Biol. Chem.* **284**, 5592-5601.
Santoro, M. M., Pesce, G. and Stainier, D. Y. (2009). Characterization of vascular mural cells during zebrafish development. *Mech. Dev.* **126**, 638-649.
Sharpe, J., Ahlgren, U., Perry, P., Hill, B., Ross, A., Hecksher-Sorensen, J., Baldock, R. and Davidson, D. (2002). Optical projection tomography as a tool for 3D microscopy and gene expression studies. *Science* **296**, 541-545.
Spiekerkoetter, E., Guignabert, C., de Jesus Perez, V., Alastalo, T. P., Powers, J. M., Wang, L., Lawrie, A., Ambartsumian, N., Schmidt, A. M., Berryman, M. et al. (2009). S100A4 and bone morphogenetic protein-2 codependently induce vascular smooth muscle cell migration via phospho-extracellular signal-regulated kinase and chloride intracellular channel 4. *Circ. Res.* **105**, 639-647.
Torihashi, S., Hattori, T., Hasegawa, H., Kurahashi, M., Ogaeri, T. and Fujimoto, T. (2009). The expression and crucial roles of BMP signaling in development of smooth muscle progenitor cells in the mouse embryonic gut. *Differentiation* **77**, 277-289.
Vastardis, H., Karimbux, N., Guthua, S. W., Seidman, J. G. and Seidman, C. E. (1996). A human MSX1 homeodomain missense mutation causes selective tooth agenesis. *Nat. Genet.* **13**, 417-421.
Walls, J. R., Coultas, L., Rossant, J. and Henkelman, R. M. (2008). Three-dimensional analysis of vascular development in the mouse embryo. *PLoS ONE* **3**, e2853.
Wiegreffe, C., Christ, B., Huang, R. and Scaal, M. (2009). Remodeling of aortic smooth muscle during avian embryonic development. *Dev. Dyn.* **238**, 624-631.
Wilkie, A. O. (1997). Craniosynostosis: genes and mechanisms. *Hum. Mol. Genet.* **6**, 1647-1656.
Yang, X., Castilla, L. H., Xu, X., Li, C., Gotay, J., Weinstein, M., Liu, P. P. and Deng, C. X. (1999). Angiogenesis defects and mesenchymal apoptosis in mice lacking SMAD5. *Development* **126**, 1571-1580.
Zhang, J., Zhong, W., Cui, T., Yang, M., Hu, X., Xu, K., Xie, C., Xue, C., Gibbons, G. H., Liu, C. et al. (2006). Generation of an adult smooth muscle cell-targeted Cre recombinase mouse model. *Arterioscler. Thromb. Vasc. Biol.* **26**, e23-e24.
Zhang, Z., Song, Y., Zhao, X., Zhang, X., Fermin, C. and Chen, Y. (2002). Rescue of cleft palate in Msx1-deficient mice by transgenic Bmp4 reveals a network of BMP and Shh signaling in the regulation of mammalian palatogenesis. *Development* **129**, 4135-4146.